

## CHAPTER 7

### THERMAL-HYDRAULIC ANALYSIS

The coolant in the pressure tube of the CANDU nuclear reactor core removes the thermal energy produced in the nuclear fuel. The rate and form of energy transfer from the nuclear fuel through the cladding and to the coolant is strongly dependent upon the local thermal and hydraulic conditions. Here we will discuss some of the thermal-hydraulic features which characterize the CANDU system.

#### 7.1 SYSTEM DESCRIPTION

The thermal-hydraulic system of a nuclear reactor possesses some features common to conventional fossil-fuel power stations. A heat source raises the temperature of a working fluid; the thermal energy thus added is subsequently converted to steam in a boiler; the steam enters a steam turbine under high pressure inducing rotational energy; the shaft of the turbine is directly connected to a generator which feeds electricity into a distribution grid; the ejected low pressure and low quality steam is subsequently condensed using river or lake water and returned to the boiler. Figure 7.1 provides a simple schematic representation of these features for the CANDU-PHW reactor.

In contrast to the two-loop CANDU-PHW system, we consider the one-loop or direct cycle of the CANDU-BLW (Boiling Light Water) system as illustrated in Fig. 7.2. In this cycle the steam which drives the turbine is generated directly in the core. Here we also note the vertical orientation of the coolant channels and that the flow is upwards. As the light water coolant passes through the core it changes from single phase to two phase.

Consider a more detailed description of the CANDU-PHW. In Fig. 7.3 we show some of the additional components of the thermal-hydraulic system for the Bruce reactors. Also shown here are some of the temperature, pressure, and flow rate parameters. Note a figure-eight configuration in this coolant loop. The fluid which passes through a distinct set of boilers and passes through the core in the opposite direction. Indeed, the coolant is made to flow in opposite directions in adjacent channels.

The primary heat transport system is characterized by the installation of two main circuits in order to reduce the rate of reactor blowdown in the event of a sudden loss of coolant. Each of the two loops contains two pumps, two boilers, and reactor inlet and outlet headers.

Four identical heat exchangers transfer heat from the reactor coolant to raise the temperature and boil feedwater. These heat exchangers consist of an inverted vertical U-tube bundle installed in a shell constructed according to the ASME Boiler and Pressure Vessel Code.

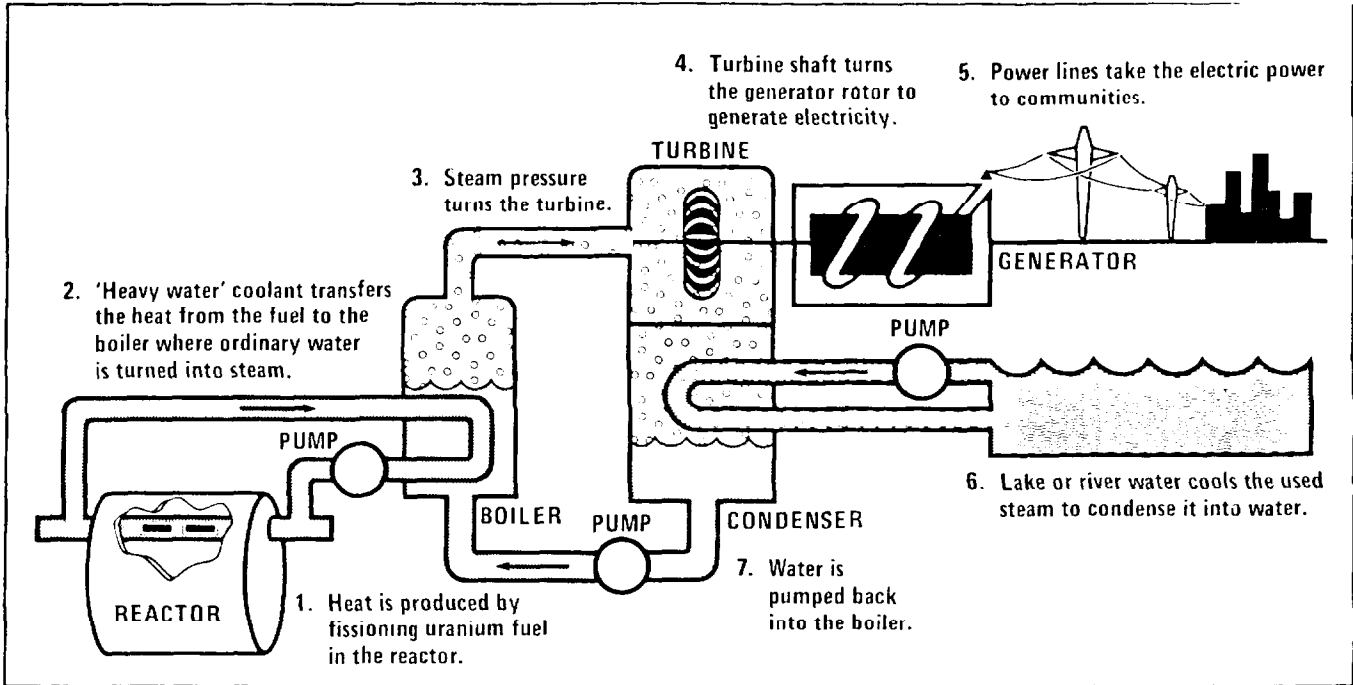


FIG. 7.1: General thermal-hydraulic features of a pressurized (PHW) CANDU reactor system.

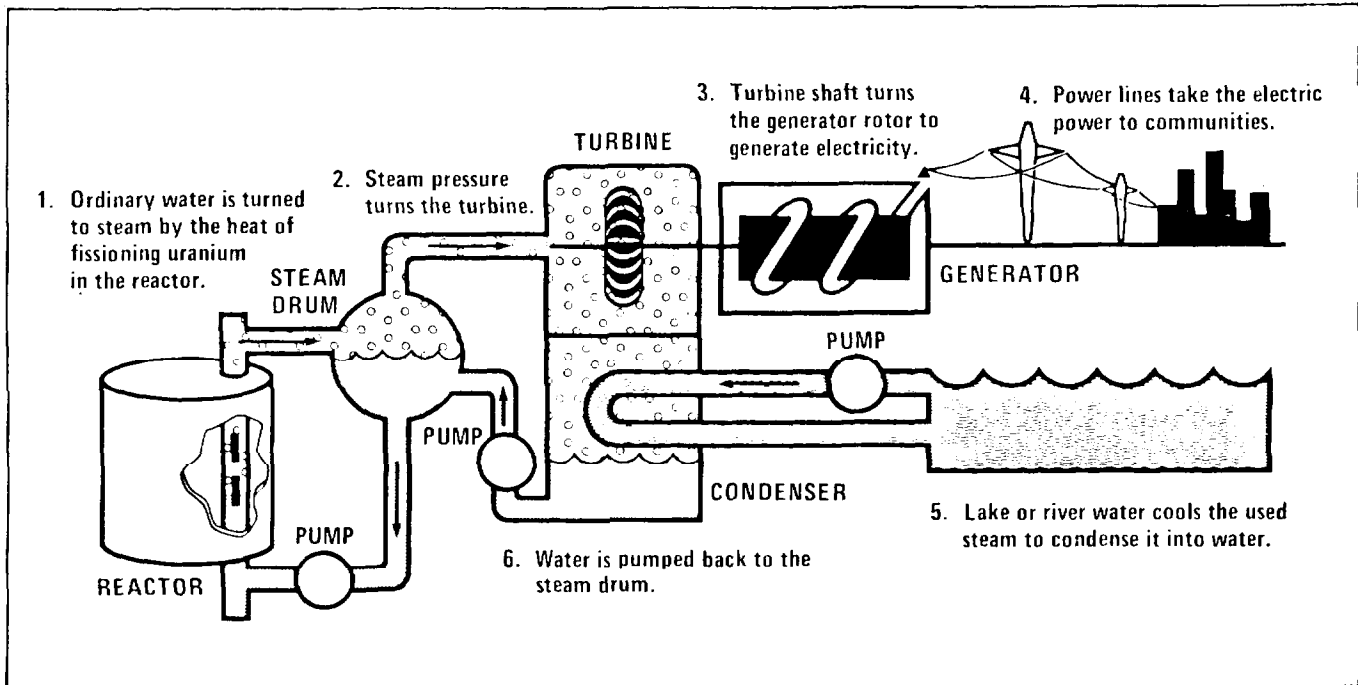


FIG. 7.2: General thermal-hydraulic features of a boiling (BLW) CANDU reactor system.



The heat transport pumps are vertical, single stage, and of the single suction double discharge centrifugal type. The shaft sealing arrangement consists of three mechanical seals and one back-up seal in series. Each mechanical seal is suitable for operating at full differential pressure and all three are housed in a removable cartridge. Each motor is also equipped with a flywheel so that the rotational energy of the pump motor unit prolongs pump operation after loss of motor power; the decreasing rate of flow approximately matches the power rundown associated with a reactor emergency shut-down. Figure 7.4 provides an isometric view of a boiler and pump system.

## 7.2 THERMAL-HYDRAULIC REGIMES

We have previously indicated that the production of fission energy in the reactor core varies as a function of axial position. In the first instance, the energy heat transfer characteristics of the coolant should relate in a direct way to this axial dependence. However, hydraulic conditions can effect the heat transfer characteristics from the nuclear fuel to the coolant in a most significant manner. We consider, therefore, some of the more pronounced thermal and hydraulic regimes in a coolant channel.

The coolant normally enters the reactor channel in its single phase condition. As the coolant flows through the channel its temperature rises and, as heat flow continues to be added from the nuclear fuel, the coolant approaches the saturation temperature corresponding to the local pressure conditions. Bubbles may form in the coolant and subsequently form slugs of voids which create large variations in the void fraction along any given channel traverse. Eventually, a single phase high steam quality condition may develop in the coolant.

Associated with these dominant changes in the thermal and hydraulic conditions of the coolant, significant changes in the sheathing temperature may also occur. Though the surface temperature will rise initially, it will remain largely constant during the bubble flow and initial slug conditions. Then, at the point in the channel when liquid deficient flow develops, the sheathing surface temperature will increase abruptly. This identifies dryout conditions and, for reasons of heat transfer and thermal effects on the sheathing, represents a most undesirable condition. These possible hydraulic and temperature regimes are graphically illustrated in Fig. 7.5.

Several important variations in the hydraulic and thermal properties of a coolant channel can be incorporated in the design. By the appropriate choice of dimensions of channels, flow velocities and designed pressure drops, it is possible to provide different axial temperature profiles and void conditions. We indicate such possibilities for the case of a very similar axial distribution of fission energy production, Fig. 7.6; the cases considered here are the pressurized system appropriate to the PHW Bruce reactors and that of the BLW Gentilly reactor.

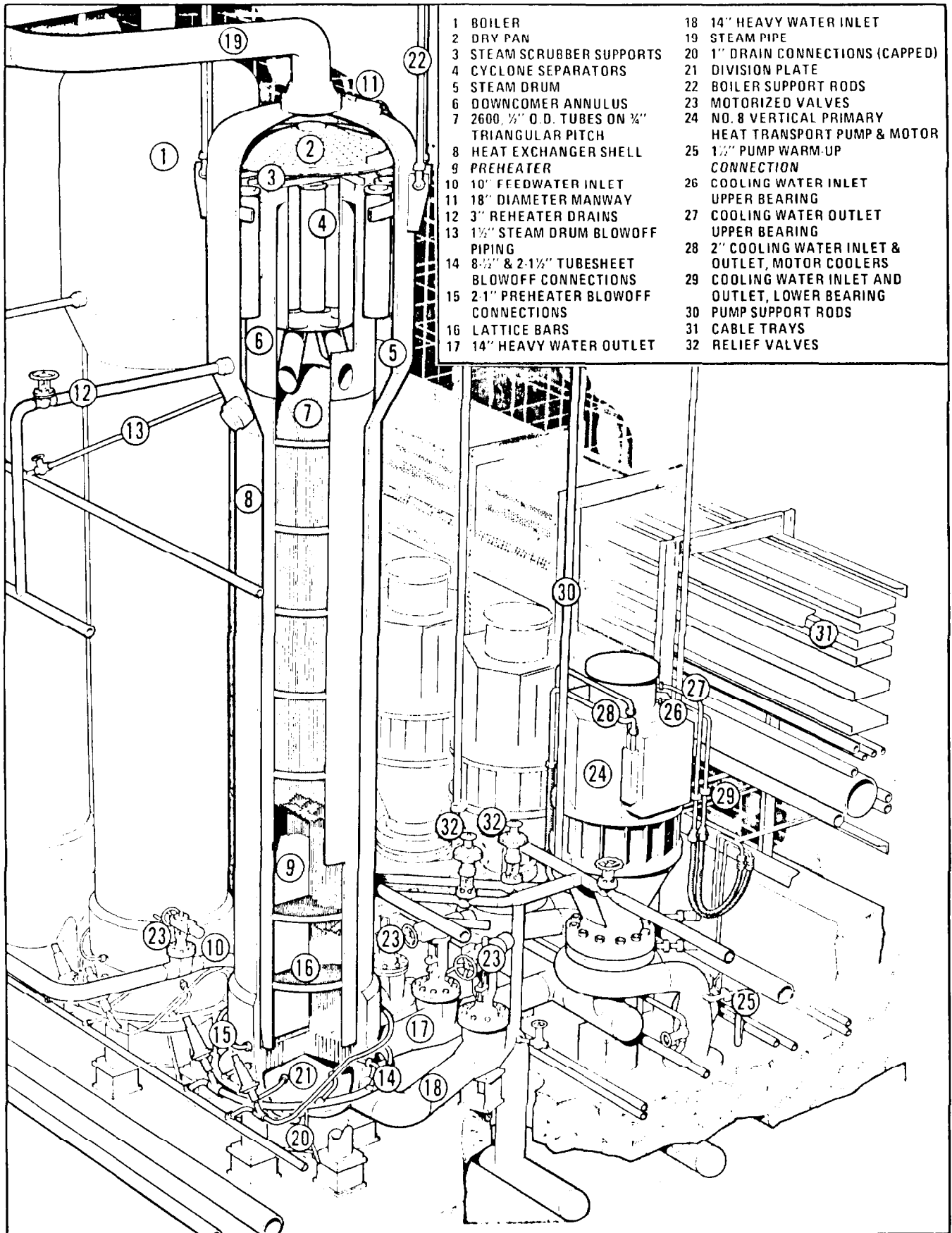


FIG. 7.4: Isometric view of boiler and pump arrangement.

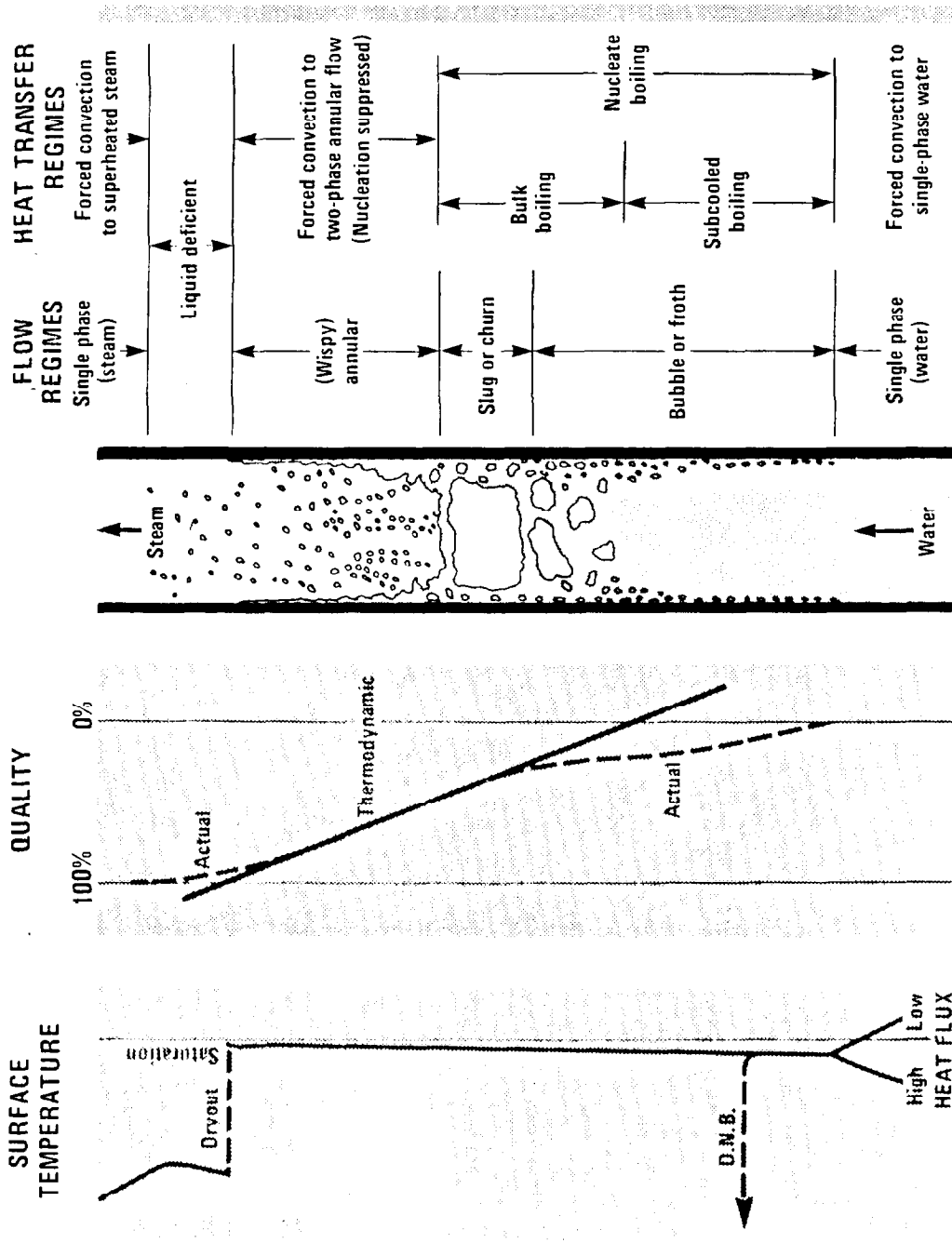


FIG. 7.5: Possible thermal-hydraulic regimes in a coolant channel.

The symmetric curve in Fig. 7.6 depicts the idealized power density appropriate to a homogeneous reactor core. Both, the sheath temperature and the coolant temperature in the pressurized heavy water reactor increases monotonically in the direction of coolant flow and reaches a maximum near the exit of the channel. The corresponding temperatures in the boiling light water reactor increase very quickly in the channel but then gradually decrease resulting in a net coolant temperature increase substantially less than that for the pressurized channel. For purpose of graphical clarity, we have not listed the temperature values in Fig. 7.6; Table 7.1 provides a listing for several Canadian reactors.

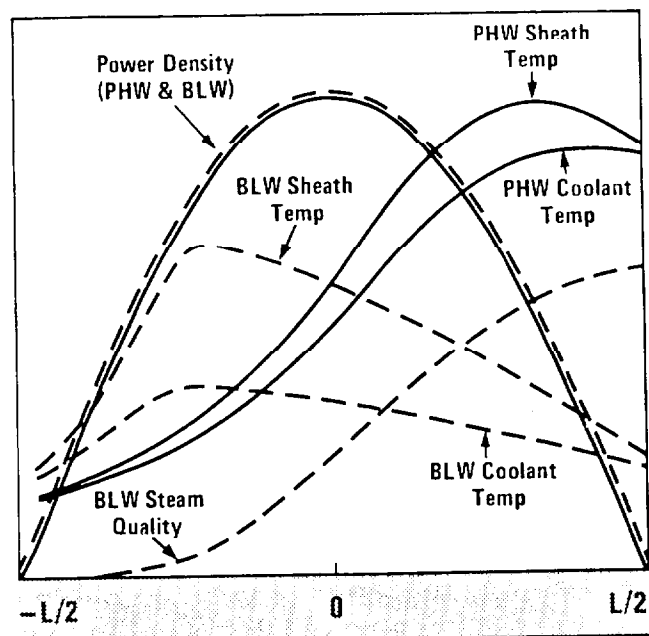


FIG. 7.6: Axial variations of the power density and temperature for a pressurized (PHW) and boiling (BLW) CANDU reactor.

Reactor	Coolant Inlet	Coolant Outlet	Temperature Increase
Douglas Point (PHW)	480°F(249°C)	560°F(293°C)	80°F(44°C)
Pickering (PHW)	480°F(249°C)	560°F(293°C)	80°F(44°C)
Gentilly (BLW)	500°F(260°C)	514°F(268°C)	14°F(8°C)
Bruce (PHW)	485°F(252°C)	570°F(299°C)	85°F(47°C)

TABLE 7.1: Temperature of coolant of several Canadian reactors.

The significant smaller difference in coolant temperature rise of the boiling reactor, Gentilly (BLW), in comparison to the pressurized reactors is worth noting.

Several important heat transfer limitations must be recognized in the thermal-hydraulic analysis of a coolant channel system. Both single phase and some two-phase flow conditions are associated with good heat transfer conditions. However, at the point where nucleate boiling yields to film boiling, a critical condition may develop where the heat transfer rate may even decrease with

increasing cladding temperature. This point corresponds to the critical heat flux, generally abbreviated CHF, and represents an important design limitation, Fig. 7.7.

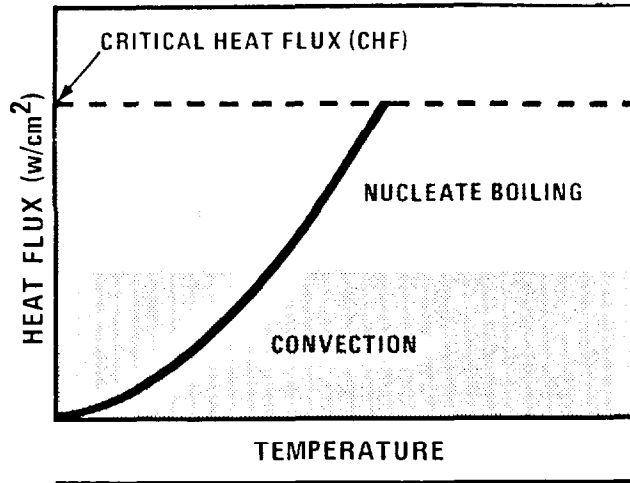


FIG. 7.7: Heat flux as a function of temperature.

The determination of the critical heat flux represents a demanding problem in heat transfer calculations. It is invariably related to such parameters as power density, flow rate, coolant pressure, channel dimensions and thermal efficiency. For example, though a higher pressure follows directly as a result of higher temperature and thus leads to higher thermal efficiency and lower energy costs, along with these considerations is the need for thicker pressure tubes and the occurrence of higher corrosion rates. This situation characterizes much of nuclear reactor design analysis: it is often a matter of balancing material and operating constraints both of which relate to the cost of the system.

### 7.3 TEMPERATURE PROFILES IN THE FUEL

The relevant steady-state heat transfer relations of importance to the determination of the radial temperature profile nuclear fuel elements are, first, conservation of energy in a cylindrical differential volume element in the fuel

$$q'''(r,z) = \nabla_{\vec{r}} \cdot \vec{q}''(r,z) , \quad (7.1)$$

and, second, Fourier's law of heat conduction

$$\vec{q}''(r,z) = -k \nabla_{\vec{r}} T(r,z) , \quad (7.2)$$

where



$T(r,z)$  = local medium temperature, °C,  
 $k$  = thermal conductivity of the medium, watt/cm<sup>2</sup>-°C,  
 $\vec{q}''(r,z)$  = vector heat flux, watt/cm<sup>2</sup>,  
 $q'''(r,z)$  = power density, watt/cm<sup>3</sup>.

The power density is zero everywhere except in the nuclear fuel region; in this fuel region it is defined in terms of the fission process as discussed in a preceding chapter:

$$q'''(r,z) = \gamma \int_0^{\infty} \Sigma_f(r,z,E) \phi(r,z,E) dE, \quad (7.3)$$

where  $\gamma$  is the constant of proportionality possessing units of watt-sec/MeV.

In the attached definition sketch, Fig. 7.8, we illustrate the material composition relevant herein for a fuel-sheath-coolant cell; here we also specify the thermal conductivities in each region and indicate the local temperatures as specific radial coordinates.

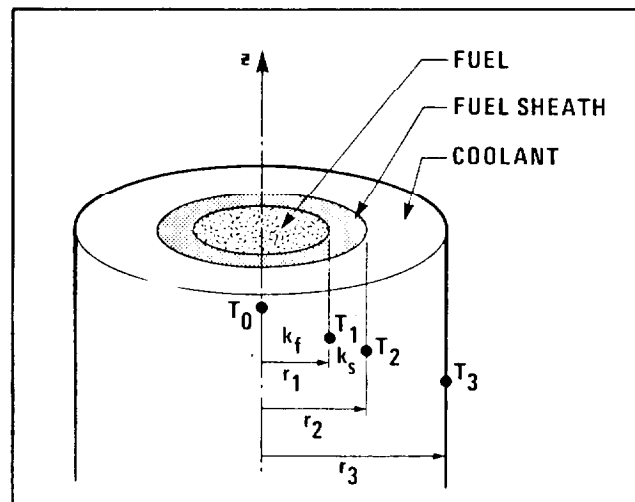


FIG. 7.8: Definition sketch used in the determination of the radial temperature profile in a fuel-sheath-channel element.

Starting our analysis in the fuel domain with Eq. (7.1) and Eq. (7.2) we write

$$q'''(r,z) = \nabla \cdot \vec{q}''(r,z) = \nabla \cdot [-k_f \nabla T_f(r,z)] . \quad (7.4)$$

Restricting our analysis to a specific  $z$ -coordinate and assuming that both the thermal conductivity,  $k_f$ , and that the nuclear power density,  $q'''$ , is a constant in the medium permits integration of this equation twice to obtain the radial fuel temperature,  $T_f(r)$ , in terms of two constants of integration. These constants

can easily be eliminated by imposing the conditions that  $T_f(r)$  is finite in the fuel and equal to  $T_1$  at the fuel sheath interface. The radial temperature of the fuel can thus be shown to be given as a quadratic function of  $r$ :

$$T_f(r) = T_1 + \frac{q'''}{4k_f} (r_1^2 - r^2) . \quad (7.5)$$

The heat flux in the radial direction is, however, linear in  $r$ :

$$q_f''(r) = -k_f \frac{dT_f(r)}{dr} = q''' \frac{r}{2} . \quad (7.6)$$

The temperature profile in the sheath can be determined in a similar manner with one simplifying property; since no energy is generated in the sheath,  $q'''(r)$  is zero in the sheath; we write Eq. (7.1)

$$\nabla \cdot \underline{q}''(r) = 0 , \quad (7.7)$$

and finally obtain

$$T_c(r) = T_1 - \frac{r_1 q_s''(r_1)}{k_s} \ln\left(\frac{r}{r_1}\right) . \quad (7.8)$$

The mean temperature in the coolant,  $T_h$ , may be represented with the aid of Newton's law of cooling by

$$q''(r_2) = h(T_2 - T_h) , \quad (7.9)$$

where  $H$  is the film coefficient of heat transfer. Hence we write

$$T_h = T_2 - \frac{q''(r_2)}{h} = T_2 - \frac{q'''}{2hr_2} r_1^2 . \quad (7.10)$$

Figure 7.9 provides a graphical representation of the radial temperature profile for a fuel element. Note that although the coolant temperature may be of the order of  $300^\circ\text{C}$ , the maximum centre-line fuel temperature may exceed  $2000^\circ\text{C}$ .

A more exact and more detailed thermal analysis will provide a temperature profile which differs in some respects from the above ideal representation. These differences may be attributed to the following factors.

1.  $k_f$  is both space dependent and temperature dependent;
2.  $q'''$  is space dependent;
3. contact resistance between the fuel and sheath;
4. boundary layer phenomena of the sheath-coolant interface.

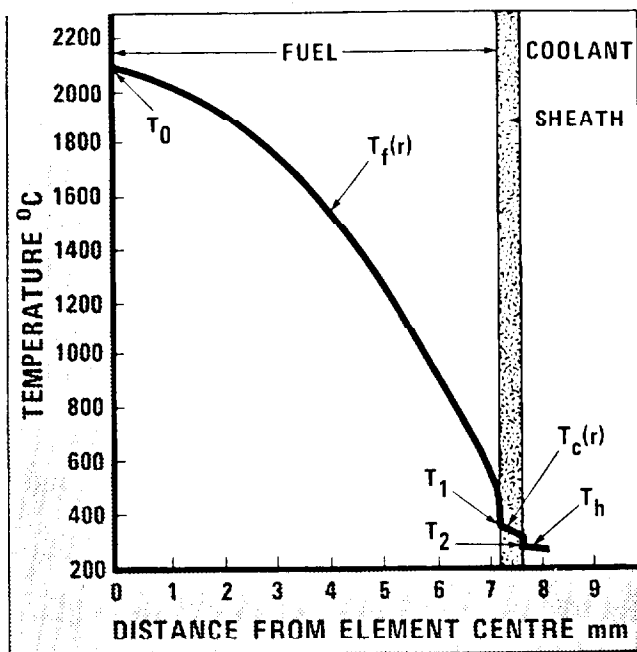


FIG. 7.9: Radial temperature profile in a fuel element.

The axial temperature profiles are determined on the basis of a similar analysis. It can be shown that the various coolant temperatures and the maximum sheath temperatures possess profiles similar to those shown in Fig. 7.6. Typical radial variations of the maximum, mean, and surface temperatures of uranium oxide fuel are shown in Fig. 7.10.

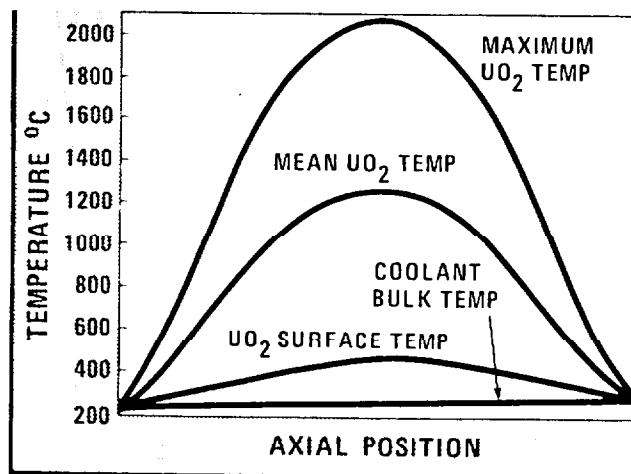


FIG. 7.10: Axial fuel temperatures of uranium oxide fuel.

